4．不妊・先天異常
4）Beckwith-Wiedemann 症候群と小児腫瘍

東元　健・副島英伸

Beckwith-Wiedemann 症候群（BWS）は，小児腫瘍を合併しやすい過成長症候群である。原因遺伝子座である 11p15.5 領域には２つの刷り込みドメインが存在し，この領域のエピジェネティックあるいはジェネティックな異常によって発症する。発症原因によって小児腫瘍の合併リスクや種類が異なることが知られている。近年，11p15.5 領域に加え，他の刷り込み制御領域にも同時にエピジェネティックな異常を生じている症例が報告されており，エピジェネティック異常の分子機構の点から注目されている。また，BWS をはじめとする刷り込み疾患と生殖補助医療との関わりが示唆されている。

はじめに

Beckwith-Wiedemann 症候群（BWS）は，新生児期の過成長，巨舌，臍ヘルニア・臍帯ヘルニアを 3 主徴とし，その他に耳垂の線状溝・耳輪後縁の小窩，新生児期低血糖，腹腔内臓腫大，腎臓奇形，片側肥大，口蓋裂などの多様な症状を呈する。また報告によって異なるが（4 ～ 21％），総じて約 7.5％の患者に Wilms 腫瘍，肝芽腫，神経芽腫などの小児腫瘍を発生する。発症原因は複数あり，11p15.5 領域のエピジェネティックな異常（DNA メチル化異常）やジェネティックな異常による刷り込み遺伝子[用解1]の発現異常あるいは機能喪失によって発症する。また，発症原因の多くを占める DNA メチル化異常と父性片親性ダイソミー（父性 UPD：paternal uniparental disomy）[用解2]は，正常細胞と異常細胞が混在するモザイク[用解3]であり，BWS 患者間ならびに同一患者の組織間でも，モザイクの割合が異なることが知られている。このため，BWS 患者の示す症状とその重症度は多様である。

本稿では，BWS の発症メカニズム，発症原因別の代表的な表現型と小児腫瘍の合併リスクならびに腫瘍の種類を示す。また最近の知見として，11p15.5 領域に加え他の刷り込み制御領域（ICR：imprinting control region）[用解4]に DNA メチル化異常を伴う BWS ならびに生殖補助医療と BWS の関連について解説する。

Ⅰ．11p15.5 領域の刷り込み遺伝子の制御機構

11p15.5 領域には，刷り込み遺伝子がクラスターをなして存在し，ドメインレベルで制御されている。2 つのドメインがあり，テロメア側から *IGF2/H19* ドメイン，*KCNQ1* ドメインと呼ばれている。また各ドメインは，刷り込み遺伝子のアレ

key words
Beckwith-Wiedemann 症候群（BWS），小児腫瘍，刷り込み遺伝子，刷り込み制御領域（ICR），メチル化可変領域（DMR），*IGF2/H19* ドメイン，*KCNQ1* ドメイン，生殖補助医療（ART），父性片親性ダイソミー（父性 UPD），マルチローカスメチル化異常

ル特異的発現を制御する刷り込み制御領域（ICR）をもつ。ICRは，親由来アレル特異的にDNAメチル化状態が異なるメチル化可変領域（DMR：differentially DNA methylated region）[用解5]を形成している。

1. *IGF2/H19* ドメイン

このドメインのICRは，*H19*上流の2～5kbにあるH19-DMRである（図❶A）。H19-DMRは，父由来アレルがDNAメチル化，母由来アレルがDNA非メチル化を示す。また，*H19*の下流には，*H19*と*IGF2*の両方のプロモーターを活性化させるエンハンサー[用解6]が存在する。H19-DMR内には複数のCTCF結合配列があるが，CTCFの結合はメチル化感受性であるため，非メチル化の母由来アレルのみに結合する。CTCFが結合するとインスレーター[用解7]として機能し，母由来アレルにおいてエンハンサーが*IGF2*プロモーターに作用することをブロックする。そのため，エンハンサーはインスレーター下流の*H19*プロモーターに作用し，転写を活性化する。一方，父由来H19-DMRはメチル化されているため，CTCFが結合できずインスレーター活性を示さない。この場合，エンハンサーは*IGF2*プロモーターに作用し，転写を活性化する。H19-DMRのメチル化は*H19*プロモーターにまで及ぶため，父由来の*H19*の発現は抑制される。その結果，*IGF2*は父性発現，*H19*は母性発現を示す[1]。上記のモデルは広く受け入れられているが，最近CTCFがクロマチンループの形成に関与すると考えられているコヒーシンと共局在を示すことがわかり，CTCF/コヒーシンによる親由来特異的クロマチンループによるモデルが提唱された。このモデルでは，クロマチンループの形成によりエンハンサーが*IGF2*あるいは*H19*のプロモーターのどちらに近接しているかによって，これら遺伝子のアレル特異的発現を調節している[2]。

2. *KCNQ1* ドメイン

このドメインのICRは，*KCNQ1*のイントロンに存在するKvDMR1である（図❶A）。KvDMR1は，母由来アレルでDNAメチル化，父由来アレルでDNA非メチル化を示す。父由来アレルの非メチル化KvDMR1はプロモーター活性をもち，*KCNQ1*と逆向きに*KCNQ1OT1*を転写させる。母由来のプロモーターはメチル化により不活化されるため，結果的に*KCNQ1OT1*は父由来アレルのみ発現する。また，この遺伝子はタンパクに翻訳されないlong non-coding RNA（lncRNA）として核内で機能する。マウスにおいて，このlncRNAは，ヘテロクロマチン[用解8]形成に関わる因子と複合体を形成することが示された。これら因子は胎盤と胎盤以外の組織で異なっており，胎盤ではポリコームタンパクPRC1, PRC2複合体とヒストンリジン9メチル化酵素G9aであり，胎盤以外の組織ではDNAメチル化酵素Dnmt1である[3)-5)]。この違いは，KvDMR1の遠方に位置する遺伝子は胎盤特異的に刷り込みを受けているのに対し，胎盤以外の組織では刷り込みを受けていないことに関係すると考えられている。*KCNQ1OT1*とヘテロクロマチン関連タンパクとの複合体は父由来染色体上でシスに作用し，周辺の刷り込み遺伝子の父由来発現を抑制する。このため，*KCNQ1OT1*以外の刷り込み遺伝子は母性発現を示す[1]。

Ⅱ. BWS発症原因別にみた表現型と小児腫瘍（表❶）

BWSは85%が孤発例で，残り15%が家族例である。BWSは様々な原因により発症するが，発症原因の多くを占めるDNAメチル化異常や父性UPDは，正常細胞と異常細胞が混在するモザイクを示す。このことから，これらの異常は受精後に生じていると考えられている[1)6)]。このモザイクの割合は，BWS患者間ならびに同一患者の組織間でも異なっており，多様な表現型の一因となっている。

1. H19-DMRの高メチル化

発症原因の約5%を占める。母由来H19-DMRが高メチル化になると，母由来アレルが父型の制御を受ける。つまり，*IGF2*は両アレル発現を示し過剰発現する。一方，*H19*は両アレル共に転写されない（図❶B）。*IGF2*はインスリン様成長因子であり，細胞分裂促進作用や抗アポトーシス作

図❶ 11p15.5 領域の刷り込みドメイン（文献 1 より改変）

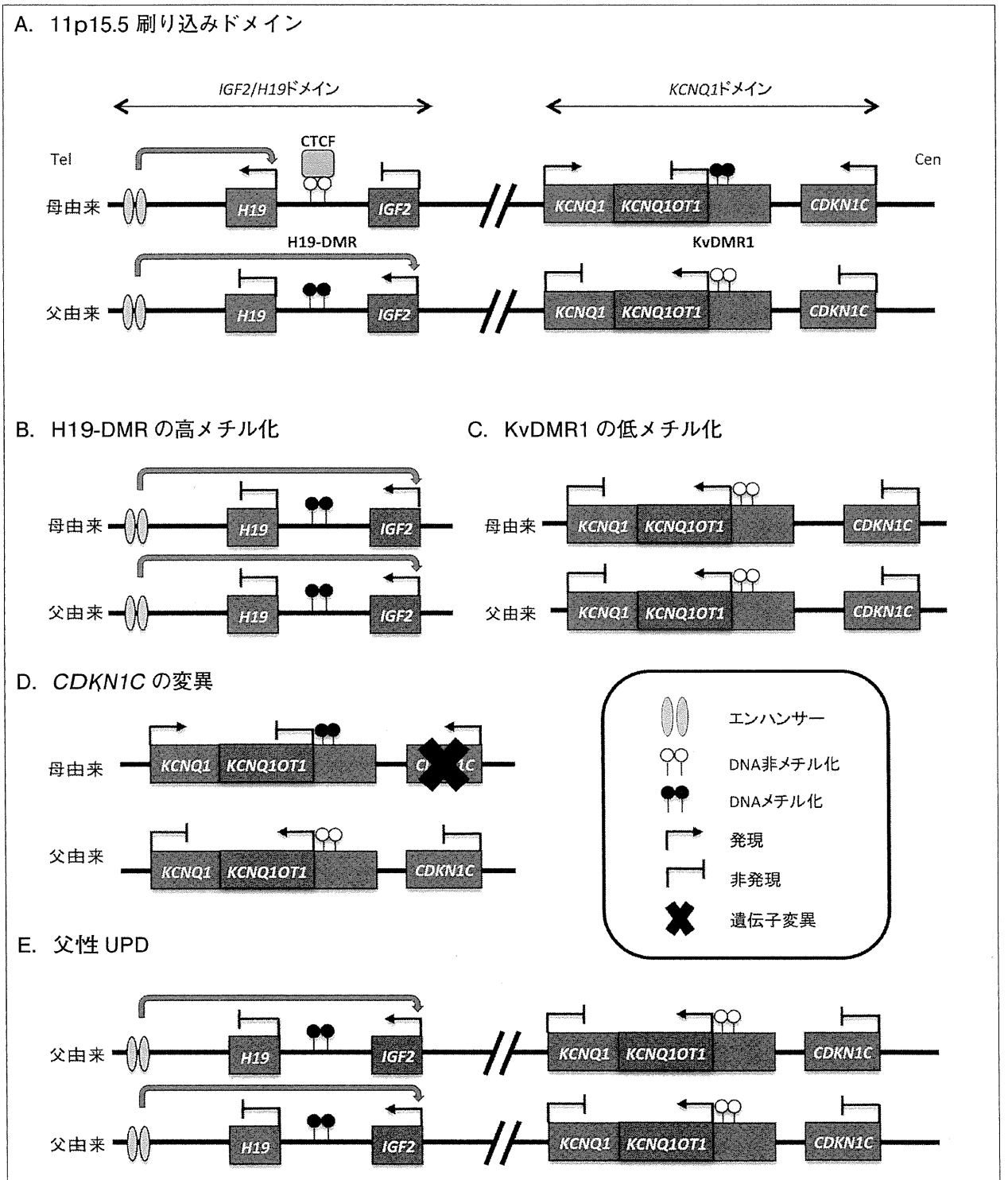

A. 11p15.5 領域の刷り込み制御機構。制御単位によって，*IGF2/H19* ドメインと *KCNQ1* ドメインの 2 つに分かれる。それぞれのドメインの ICR は，H19-DMR と KvDMR1 である。赤は母性発現，青は父性発現する刷り込み遺伝子である。詳細は本文参照。
B. H19-DMR の高メチル化。母由来 H19-DMR の高メチル化によって，母由来アレルが父型の制御を受ける。
C. KvDMR1 の低メチル化。母由来 KvDMR1 の低メチル化によって，母由来アレルが父型の制御を受ける。
D. *CDKN1C* の変異。母由来アレルの *CDKN1C* に変異があるとき，BWS を発症する。
E. 父性 UPD。*IGF2/H19* ドメインと *KCNQ1* ドメインともに父由来である。 （グラビア頁参照）

表❶　BWS 発症原因別の代表的表現型と小児腫瘍（文献 1 より改変）

発症原因	頻度	代表的表現型	小児腫瘍発生のリスク	小児腫瘍の種類
H19-DMR 高メチル化	5%	片側肥大	>25%	Wilms 腫瘍 肝芽腫
KvDMR1 低メチル化	50%	臍ヘルニア 片側肥大	<5%	肝芽腫 横紋筋肉腫など （Wilms 腫瘍以外）
CDKN1C 変異	10%	口蓋裂 臍ヘルニア	<5%	神経芽腫
父性 UPD	20%	片側肥大	>25%	Wilms 腫瘍 肝芽腫
転座・逆位	1%	報告は少ないが典型的表現型を示す	—	—
11p15 重複	1%	発育遅延	—	—

用を有する。その過剰発現は，BWS 発症や様々な腫瘍発生の中心的な役割を担うと考えられている[1]。一方，*H19* はマウスにおけるその機能喪失が BWS 様表現型を示さないこと，また当初は腫瘍抑制遺伝子として報告されていたが，様々な腫瘍でその発現が上昇していることから，その機能はよくわかっていない[7]。多くの H19-DMR 高メチル化を示す患者はジェネティックな異常を伴わないが，その約 20%において母由来 H19-DMR 内に，CTCF 結合配列を含む微小欠失，また着床後の母由来 H19-DMR の非メチル化の維持に重要である OCT 結合配列の変異や欠失が認められる[8]。H19-DMR 高メチル化異常による BWS は，小児腫瘍合併のリスクが >25%と顕著に高い。また腫瘍の種類は，Wilms 腫瘍や肝芽腫が多い[1]。実際，当研究室での孤発例の Wilms 腫瘍の解析において，*IGF2* の両アレル発現を示す割合は 40%と非常に高かった[9]。また，ヒト大腸がんと *IGF2* の両アレル発現の関連はよく知られている。ヒト大腸がんのモデルである *Apc* 遺伝子変異マウスにおける *Igf2* の両アレル発現は，*Igf2* が正常に発現しているものに比べて腺腫発生率が有意に高くなる[10]。最近，*H19* 領域に *H19* とは反対向きに転写され，母由来アレル特異的に発現する *HOTS* という刷り込み遺伝子が見つかった。この遺伝子は，*H19* とは異なりタンパクをコードする。この HOTS は Wilms 腫瘍などの小児腫瘍細胞株で腫瘍抑制活性を示し，その発現は *IGF2* の両アレル発現を示すすべての Wilms 腫瘍で消失していた[7]。これらの事実は，*IGF2* の両アレル発現以外の H19-DMR 高メチル化が関連する腫瘍発生機序の存在を示唆している。

2. KvDMR1 の低メチル化

発症原因の約 50%を占める。母由来 KvDMR1 のメチル化が喪失すると，母由来アレルが父型の制御を受ける。つまり，母由来アレルでも *KCNQ1OT1* が発現し，*CDKN1C*，*KCNQ1* をはじめとする周辺の遺伝子の母由来発現を抑制する（**図❶C**）。このドメインで BWS 発症の中心的な役割を担う遺伝子は *CDKN1C* である[1]。この遺伝子は細胞増殖を負に制御する CDK インヒビターをコードしており，細胞の増殖や分化を制御する。*Cdkn1c* 欠損マウスは，BWS にみられる腹壁欠損による臍ヘルニア，口蓋裂，腎髄質の異形成や副腎の過形成を示す[11]。1 例の *NLRP2* の変異による KvDMR1 低メチル化を除いて，KvDMR1 低メチル化がジェネティックな異常によって起こる例は報告されていない[12]。この KvDMR1 低メチル化による BWS 患者に関連する代表的な表現型は，臍ヘルニアである。一方，小児腫瘍合併リスクは <5%と低い（健常児と比べると高い）。また腫瘍の種類は，Wilms 腫瘍以外の肝芽腫や横紋筋肉腫などが報告されている[1]。

3. *CDKN1C* の変異

発症原因の約 10%を占める。BWS 家族例に限ると 40%に *CDKN1C* の変異が見つかる。*CDKN1C* は母性発現を示すため，大部分の症例では母親から変異を受け継いでいるが，稀に母由

来アレルに *de novo* の変異が生じることもある（図❶D）[13][14]。*CDKN1C* 変異患者の代表的な表現型は，*Cdkn1c* 欠損マウスにみられた表現型である臍ヘルニアと口蓋裂である。一方，小児腫瘍合併リスクは <5％で，今までに神経芽腫が報告されている[1]。CDK インヒビターである *CDKN1C* は，成人のがんでは腫瘍抑制遺伝子として働いていることが示唆されている[15]。しかしながら，*CDKN1C* の発現低下を引き起こす KvDMR1 低メチル化や *CDKN1C* の変異による BWS では，小児腫瘍合併リスクは低い。ヒトにおいて *CDKN1C* は，マウスとは異なり父由来アレルからも少し発現していることが知られている。また，いくつかの研究グループは 11p15 領域の母由来の loss of heterozygosity（LOH）を伴う Wilms 腫瘍でも，正常組織に比べ *CDKN1C* の顕著な発現低下を認めなかったと報告している[16][17]。これらのことは，*CDKN1C* と Wilms 腫瘍発生との関連性が低いことを示しているのかもしれない。

4. 父性片親性ダイソミー（父性 UPD）

発症原因の約 20％を占める。体細胞モザイクを示すことから，受精後の体細胞組換えによって生じると考えられている。父性 UPD では，父由来アレルの 11p15.5 領域が 2 コピー存在し，母由来アレルはない。ダイソミーを含む領域は，*IGF2/H19* ドメインと *KCNQ1* ドメインの両方を含むため，*IGF2* の過剰発現ならびに *CDKN1C* の発現低下を生じる（図❶E）。父性 UPD よる BWS 患者に関連する代表的な表現型は片側肥大である。一方，小児腫瘍合併リスクは，H19-DMR 高メチル化と同様に >25％と顕著に高い。また腫瘍の種類は，Wilms 腫瘍や肝芽腫が多い[1]。

5. 転座・逆位

発症原因の約 1％を占める。*KCNQ1* ドメインに存在する *KCNQ1* は，心臓を除くほとんどの組織で母由来発現を示す刷り込み遺伝子であり，また心疾患である QT 延長症候群の原因遺伝子でもある。この遺伝子内に 5 ヵ所の転座切断点が報告されており，母由来アレルにおいて転座・逆位が起こるとき，BWS を発症する。しかしながら，KvDMR1 のメチル化は正常を示し，その発症メカニズムはよくわかっていない。典型的な BWS 表現型を示すが，現在までに腫瘍の合併に関しては報告されていない[1][18]。

6. 11p15 領域の重複

発症原因の約 1％を占める。11p15 領域の重複が父由来のとき，BWS を発症する。この原因による BWS 患者に関連する代表的な表現型は発育遅延である[1]。

7. *KCNQ1OT1* 転写領域を含む微小欠失

極めて稀な発症原因として，KvDMR1 と *KCNQ1OT1* 転写領域を含む微小欠失（～ 250kb と 330kb）が 2 例報告されている[19]。これら欠失領域には *CDKN1C* は含まれていない。この欠失が母由来アレルに生じるとき，*CDKN1C* の発現が減少することが知られている。この発症メカニズムはよくわかっていないが，その欠失領域内に未同定の *CDKN1C* のエンハンサーが存在すると考えられている。報告例が少ないため，関連する表現型ならびに小児腫瘍の発生リスクに関しては不明である。

Ⅲ. マルチローカスメチル化異常を伴う BWS

近年，BWS の一部の患者において，11p15.5 領域に加えて，他の ICR においてもメチル化異常を生じている（マルチローカスメチル化異常）症例が報告されている。

1. KvDMR1 低メチル化とマルチローカスメチル化異常

KvDMR1 の低メチル化を示す BWS 症例のうち，約 20％は 11p15.5 領域以外の ICR にも低メチル化を生じていることが報告された。この低メチル化を起こしているすべての ICR は，正常では母由来アレルがメチル化されている ICR であり，父由来アレルがメチル化されている ICR はなかった[1]。また，最も低メチル化を引き起こしやすい ICR として，*NESPAS* と *GNAS* の ICR が，続いて *MEST*，*PLAGL1*，*IGF2R* の ICR が報告された[20]。このようなマルチローカスメチル化異常を伴う症例と KvDMR1 低メチル化のみを伴う症例の両群間で表現型が比較されたが，その結果は研

究グループによって異なっている。Rossignolらは，両群間に表現型の違いはないと報告した[21]。一方，Bliekらは，マルチローカスメチル化異常を伴うBWSのほうが出生時体重が小さく，通常BWSの表現型としてみられない言語遅滞や聴音障害を合併する例があることを報告した[20]。また，小児腫瘍発生のリスクに関しては，両群間に差がないと報告している。

2. 全ゲノム父性UPD

これまでに，全ゲノム父性UPD（すべての染色体が父性UPD）のモザイク症例が8例ほど報告されている。全ゲノム父性UPDでは，すべてのICRにメチル化異常が検出され，すべての刷り込み遺伝子に発現異常を生じると考えられる。その結果，刷り込み関連疾患であるBWS，Angelman症候群，一過性新生児糖尿病などでみられる表現型を部分的に呈する。腫瘍合併は8例中3例(35%)と高く，Wilms腫瘍，肝芽腫，両側性褐色細胞腫が報告されている[22]。

Ⅳ．生殖補助医療（ART）とBWS

生殖補助医療（ART：assisted reproductive technology）による出生児は，自然妊娠での出生児に比べ刷り込み関連疾患の発症頻度が高いことが知られている。BWSでは，ARTによる出生頻度は自然妊娠に対して約4倍から9倍高いと報告されている。ARTによって出生したBWS患者のほとんどすべてがKvDMR1の低メチル化を示す。Limらは，ARTによるBWSと自然妊娠例のKvDMR1低メチル化によるBWSと比較した結果，ARTによるBWSのほうが，臍ヘルニアを伴う頻度が少ないこと，小児腫瘍の発生リスクが高いこと，マルチローカスメチル化異常を伴う頻度が高いことを報告した[23]。

おわりに

BWSの発症原因の多くが，DNAメチル化異常によるものである。現在のところ，ほとんどのメチル化異常は，確率論的に偶発する，あるいは環境因子によって誘発されるエピジェネティックなエラーによって説明される。これらメチル化異常は，ほとんどが子へ伝達されないことを考えると，これらの説明は妥当かもしれない。しかしながら，KvDMR1低メチル化症例において*NLRP2*の変異が見つかったように，他のトランス因子の変異がメチル化異常に関与している可能性は否定できない。また，臨床学的にBWSと診断されても，11p15.5領域に異常のない症例が15%ほどある。これらの症例でも11p15.5領域以外の異常が関与している可能性を否定できない。年々進化する次世代シークエンサーやDNAメチル化アレイによる網羅的解析により，新たな異常と原因因子が見出され，さらなる発症メカニズムの解明が期待される。

用語解説

1. **刷り込み遺伝子**：インプリンティング遺伝子とも呼ばれる。一対の対立遺伝子のうち，一方の遺伝子がその親由来に従って発現することをゲノム刷り込みといい，このような遺伝子を刷り込み遺伝子という。刷り込みを受けていない一般的な遺伝子は，その親由来にかかわらず両方のアレルが偏りなく同等に発現している。
2. **片親性ダイソミー（UPD：uniparental disomy）**：一対の相同染色体が片親から由来する場合をいう。2本とも父親由来のときは父性片親性ダイソミー，母親由来のときは母性片親性ダイソミーという。問題の染色体が両親共に減数分裂で不分離をきたし，0（ゼロ）染色体の配偶子と2染色体の配偶子が受精して生じる場合と，体細胞分裂の際に生じる場合がある。BWSでは発生初期の体細胞分裂時に体細胞組換えが生じ，11pの部分的な父性ダイソミーとなる。このためモザイクを示す。
3. **モザイク**：単一の接合子に由来し，個体の中に2種類以上の遺伝的に異なる細胞が存在する状態のことをいう。モザイクは，受精後の遺伝的変化よって起こる。この遺伝的変化には，遺伝子の変異や染色体の数的あるいは構造変化などが一般的に挙げられるが，現在ではエピジェネティックな変化も含まれる。
4. **刷り込み制御領域（ICR：imprinting control region）**：多くの刷り込み遺伝子はクラスターを形成して存在し，ドメインレベルで制御されている。このドメインレベルでの制御に中枢的役割をするDNA領域のことをいう。このような領域は，一方の親の配偶子でのみDNAメチル化を受け，受精後もそのメチル化は維持されるため，メチル化可変領域を形成している。

5. **メチル化可変領域（DMR：differentially DNA methylated region）**：親由来で異なるDNAメチル化をもつDNA領域のことをいう。
6. **エンハンサー**：特定の遺伝子のプロモーターと相互作用することにより，その遺伝子の転写活性を促進するシス作用性のDNA配列のことをいう。
7. **インスレーター**：DNAにおいて，2つの機能ドメインの障壁として働く領域のことをいう。例えば，プロモーターとエンハンサーの間にインスレーターが存在する場合，インスレーターが障壁として働くためエンハンサーはプロモーターに作用できない。
8. **ヘテロクロマチン**：高度に凝縮し，遺伝子の転写活性がほとんどみられないクロマチン領域のことをいう。

参考文献

1）Choufani S, Shuman C, et al：Am J Med Genet C Semin Med Genet 154C, 343-354, 2010.
2）Nativio R, Sparago A, et al：Hum Mol Genet 20, 1363-1374, 2011.
3）Pandey RR, Mondal T, et al：Mol Cell 32, 232-246, 2008.
4）Terranova R, Yokobayashi S, et al：Dev Cell 15, 668-679, 2008.
5）Mohammad F, Mondal T, et al：Development 137, 2493-2499, 2010.
6）Higashimoto K, Nakabayashi K, et al：Am J Med Genet A 158A, 1670-1675, 2012.
7）Onyango P, Feinberg AP：Proc Natl Acad Sci USA 108, 16759-16764, 2011.
8）Demars J, Shmela ME, et al：Hum Mol Genet 19, 803-814, 2010.
9）Satoh Y, Nakadate H, et al：Br J Cancer 95, 541-547, 2006.
10）Kaneda A, Feinberg AP：Cancer Res 65, 11236-11240, 2005.
11）Zhang P, Liégeois NJ, et al：Nature 387, 151-158, 1997.
12）Meyer E, Lim D, et al：PLoS Genet 5, e1000423, 2009.
13）Romanelli V, Belinchón A, et al：Am J Med Genet A 152A, 1390-1397, 2010.
14）Yatsuki H, Higashimoto K, et al：Genes Genom 35, 141-147, 2013.
15）Kikuchi T, Toyota M, et al：Oncogene 21, 2741-2749, 2002.
16）Taniguchi T, Okamoto K, et al：Oncogene 14, 1201-1206, 1997.
17）Soejima H, McLay J, et al：Lab Invest 78, 19-28, 1998.
18）Lee MP, DeBaun MR, et al：Proc Natl Acad Sci USA 96, 5203-5208, 1999.
19）Algar E, Dagar V, et al：PLoS One 6, e29034, 2011.
20）Bliek J, Verde G, et al：Eur J Hum Genet 17, 611-619, 2009.
21）Rossignol S, Steunou V, et al：J Med Genet 43, 902-907, 2006.
22）Inbar-Feigenberg M, Choufani S, et al：Am J Med Genet A 161A, 13-20, 2013.
23）Lim D, Bowdin SC, et al：Hum Reprod 24, 741-747, 2009.

参考ホームページ

・OMIM（Online Mendelian Inheritance in Man）#130650
Beckwith-Wiedemann syndrome；BWS
http：//omim.org/entry/130650

東元　健
1997年　九州歯科大学歯学部歯学科卒業
2002年　佐賀医科大学大学院医学系研究科博士課程修了
佐賀医科大学分子生命科学講座分子遺伝学助手
2005年　University of Wisconsin-Madison 留学
2007年　佐賀大学医学部分子生命科学講座分子遺伝学・エピジェネティクス分野助教

Research

Genome-wide parent-of-origin DNA methylation analysis reveals the intricacies of human imprinting and suggests a germline methylation-independent mechanism of establishment

Franck Court,[1,15] Chiharu Tayama,[2,15] Valeria Romanelli,[1,15] Alex Martin-Trujillo,[1,15] Isabel Iglesias-Platas,[3] Kohji Okamura,[4] Naoko Sugahara,[2] Carlos Simón,[5] Harry Moore,[6] Julie V. Harness,[7] Hans Keirstead,[7] Jose Vicente Sanchez-Mut,[8] Eisuke Kaneki,[9] Pablo Lapunzina,[10] Hidenobu Soejima,[11] Norio Wake,[9] Manel Esteller,[8,12,13] Tsutomu Ogata,[14] Kenichiro Hata,[2] Kazuhiko Nakabayashi,[2,16,17] and David Monk[1,16,17]

[1–14][Author affiliations appear at the end of the paper.]

Differential methylation between the two alleles of a gene has been observed in imprinted regions, where the methylation of one allele occurs on a parent-of-origin basis, the inactive X-chromosome in females, and at those loci whose methylation is driven by genetic variants. We have extensively characterized imprinted methylation in a substantial range of normal human tissues, reciprocal genome-wide uniparental disomies, and hydatidiform moles, using a combination of whole-genome bisulfite sequencing and high-density methylation microarrays. This approach allowed us to define methylation profiles at known imprinted domains at base-pair resolution, as well as to identify 21 novel loci harboring parent-of-origin methylation, 15 of which are restricted to the placenta. We observe that the extent of imprinted differentially methylated regions (DMRs) is extremely similar between tissues, with the exception of the placenta. This extra-embryonic tissue often adopts a different methylation profile compared to somatic tissues. Further, we profiled all imprinted DMRs in sperm and embryonic stem cells derived from parthenogenetically activated oocytes, individual blastomeres, and blastocysts, in order to identify primary DMRs and reveal the extent of reprogramming during preimplantation development. Intriguingly, we find that in contrast to ubiquitous imprints, the majority of placenta-specific imprinted DMRs are unmethylated in sperm and all human embryonic stem cells. Therefore, placental-specific imprinting provides evidence for an inheritable epigenetic state that is independent of DNA methylation and the existence of a novel imprinting mechanism at these loci.

[Supplemental material is available for this article.]

Genomic imprinting is a form of epigenetic regulation that results in the expression of either the maternally or paternally inherited allele of a subset of genes (Ramowitz and Bartolomei 2011). This imprinted expression of transcripts is crucial for normal mammalian development. In humans, loss-of-imprinting of specific loci results in a number of diseases exemplified by the reciprocal growth phenotypes of the Beckwith-Wiedemann and Silver-Russell syndromes, and the behavioral disorders Angelman and Prader-Willi syndromes (Kagami et al. 2008; Buiting 2010; Choufani et al. 2010; Eggermann 2010; Kelsey 2010; Mackay and Temple 2010). In addition, aberrant imprinting also contributes to multigenic disorders associated with various complex traits and cancer (Kong et al. 2009; Monk 2010).

Imprinted loci contain differentially methylated regions (DMRs) where cytosine methylation marks one of the parental alleles, providing *cis*-acting regulatory elements that influence the allelic expression of surrounding genes. Some DMRs acquire their allelic methylation during gametogenesis, when the two parental genomes are separated, resulting from the cooperation of the de novo methyltransferase DNMT3A and its cofactor DNMT3L (Bourc'his et al. 2001; Hata et al. 2002). These primary, or germline imprinted DMRs are stably maintained throughout somatic development, surviving the epigenetic reprogramming at the oocyte-to-embryo transition (Smallwood et al. 2011; Smith et al. 2012). To confirm that an imprinted DMR functions as an imprinting control region (ICR), disruption of the imprinted expression upon genetic deletion of that DMR, either through experimental targeting in mouse or that which occurs spontaneously in humans, is required. A subset of DMRs, known as secondary DMRs, acquire methylation during development and are regulated by nearby germline DMRs in a hierarchical fashion (Coombes et al. 2003; Lopes et al. 2003; Kagami et al. 2010).

[15]These authors contributed equally to this work.
[16]These authors jointly directed this work.
[17]Corresponding authors
E-mail nakabaya-k@ncchd.go.jp
E-mail dmonk@idibell.cat
Article published online before print. Article, supplemental material, and publication date are at http://www.genome.org/cgi/doi/10.1101/gr.164913.113.

24:554–569 Published by Cold Spring Harbor Laboratory Press; ISSN 1088-9051/14; www.genome.org

With the advent of large-scale, base-resolution methylation technologies, it is now possible to discriminate allelic methylation dictated by sequence variants from imprinted methylation. Yet our knowledge of the total number of imprinted DMRs in humans, and their developmental dynamics, remains incomplete, hampered by genetic heterogeneity of human samples.

Here we present high-resolution mapping of human imprinted methylation. We performed whole-genome-wide bisulfite sequencing (WGBS) on leukocyte-, brain-, liver-, and placenta-derived DNA samples to identify partially methylated regions common to all tissues consistent with imprinted DMRs. We subsequently confirmed the partial methylated states in tissues using high-density methylation microarrays. The parental origin of methylation was determined by comparing microarray data for DNA samples from reciprocal genome-wide uniparental disomy (UPD) samples, in which all chromosomes are inherited from one parent (Lapunzina and Monk 2011), and androgenetic hydatidiform moles, which are created by the fertilization of an oocyte lacking a nucleus by a sperm that endoreduplicates. The use of uniparental disomies and hydatidiform moles meant that our analyses were not subjected to genotype influences, enabling us to characterize all known imprinted DMRs at base-pair resolution and to identify 21 imprinted domains, which we show are absent in mice. Lastly, we extended our analyses to determine the methylation profiles of all imprinted DMRs in sperm, stem cells derived from parthenogenetically activated metaphase-2 oocyte blastocytes (phES) (Mai et al. 2007; Harness et al. 2011), and stem cells (hES) generated from both six-cell blastomeres and the inner cell mass of blastocysts, delineating the extent of embryonic reprogramming that occurs at these loci during human development.

Results

Characterization of parent-of-origin methylation profiles in human tissues using high-resolution approaches

We combined whole-genome bisulfite sequencing with Illumina Infinium HumanMethylation 450K BeadChip arrays to generate methylation profiles. To validate this approach, we compared the DNA methylation profiles generated by each method. Methylation scores produced by the two methods are very similar when the same DNA samples were assessed by both techniques (linear regression WGBS vs. Infinium array: leukocytes $R^2 = 0.92$; brain $R^2 = 0.91$; placenta $R^2 = 0.92$) (Supplemental Fig. S1). To determine the similarity between normal biparental leukocytes and those from reciprocal genome-wide UPDs, we compared the methylation values obtained from the Infinium array. This revealed high correlations between samples, indicating that the DNAs were similar, differing only at imprinted loci (linear regression: leukocytes vs. leukocytes R^2 = 0.95–0.98; mean control leukocytes vs. mean pUPD $R^2 = 0.98$; mean control leukocytes vs. mUPD $R^2 = 0.98$; mUPD vs. mean pUPD $R^2 = 0.97$; F-statistics $P < 0.001$).

Before we attempted to discover novel imprinted DMRs in the human genome, we wished to determine the effectiveness of the Infinium array to identify known imprinted DMRs. Loci were identified which contained at least three Infinium probes with an average minimal difference of 0.3 β-values (absolute methylation difference >30%) between reciprocal genome-wide UPD leukocyte samples, and with a prerequisite that the β-values for normal leukocytes should be between these extremes. Using these criteria, we identified 818 windows that could be merged into 145 regions harboring 576 probes incorporating 30 known DMRs within 25 imprinted domains (Table 1; Fig. 1A) (Limma linear model $P < 0.05$), and presented an intermediate methylation profile in all somatic tissues (Fig. 1B). The only imprinted DMRs not found using this approach were the IG-DMR located between *MEG3* and *DLK1* on chromosome 14, as this region does not have probes on this array platform and *IGF2*-DMR0 only contains a single probe.

Identification of new DMRs within known imprinted domains

In addition to the known imprinted DMRs, the Infinium array screen of reciprocal UPDs and tissues samples uncovered several previously unidentified DMRs located within existing imprinted domains. We discovered four maternally methylated CpG islands located between the *SNRPN* and *NDN* genes on chromosome 15, a region associated with the Angelman and Prader-Willi syndromes. The methylation profiles at the *SNRPN, NDN,* and *MAGEL2* promoters are well-established (El-Maarri et al. 2001; Sharp et al. 2010). However, little is known about the intervening ~1-Mb gene-poor region, which is likely to have arisen from an ancient duplication event, since these novel DMRs share 97.8% sequence identity with additional CpG-rich regions in the interval. We confirm the maternal methylation at these four regions using bisulfite PCR and sequencing, incorporating heterozygous SNPs in brain and leukocyte DNA (Supplemental Fig. S2A). Further analysis of this region revealed that the promoter region for *MKRN3* and *MIR4508* are also differentially methylated.

Extending our analysis to imprinted domains on other autosomes, we identified an ~600-bp interval of maternal methylation 4 kb 3′ from the *ZNF597* gene (Fig. 1C). Although the promoter of *ZNF597* is a paternally methylated bidirectional silencer presumably responsible for regulating the imprinted expression of both *ZNF597* and *NAA60* (previously known as *NAT15*), this region is unlikely to be the ICR for the domain as its methylation is somatically acquired (Nakabayashi et al. 2011). In addition, WGBS and Infinium array data sets revealed a maternally methylated DMR within intron 2 of *MEG8* within the chromosome 14 imprinted domain (Supplemental Fig. S2B). Lastly, we identify two maternally methylated regions. The first is an ~1-kb CpG island overlapping the promoter of isoform 3 of the *ZNF331* gene, and the second coincides with exon 2 of *DIRAS3* (Supplemental Fig. S2C).

Genome-wide methylation profiling identifies novel imprinted domains

To determine if there are additional imprinted DMRs in the human genome, we screened for regions of intermediate methylation common to lymphocyte, brain, and liver WGBS data sets. Using a sliding window approach that takes into account 25 consecutive CpG sites and following removal of class 1 transposable elements (LINEs, *Alu*/SINEs, and LTR elements) and satellite DNA, we identified 356 nonoverlapping, single-copy regions in pairwise comparisons of tissues, of which 63 loci were common to the all tissues ($0.25 < \text{mean} \pm 1.5\ \text{SD} < 0.75$) (Fig. 2A; Supplemental Table S1).

A screen for three consecutive partially methylated probes in leukocyte, brain, liver, kidney, and muscle Infinium data sets, with a profile consistent with parent-of-origin methylation in the reciprocal UPD leukocyte samples, identified 116 regions (Supplemental Table S1). By combining the 356 regions detected by WGBS and the 116 loci identified by the Infinium array, we identified 64 regions in common, which included all known imprinted DMRs and 17 CpG-rich sequences possessing a methylation profile consistent with imprinting. Using standard bisulfite PCR, we assessed

Table 1. Location of parent-of-origin methylation identified in this study

Known imprinted DMRs (n = 36)								Novel DMRs (n = 25)							
		Extent (WGBS)						Novel DMRs near known imprinted loci (n = 8)							
Gene locus	Chr	Start	Finish	# Infinium probes	GC content	# CpG	Methylation origin	Gene locus	Chr	Extent (WGBS) Start	Finish	# Infinium probes	GC Content	# CpG	Methylation origin
DIRAS3	1	68515433	68517545	17	0.50	88	M	*DIRAS3* Ex2	1	68512505	68513486	8	0.52	39	M
ZDBF2	2	207114583	207136544	8	0.45	439	P	*MEG8*	14	101370741	101371419	1	0.66	43	M
NAP1L5	4	89618184	89619237	15	0.57	57	M	*SNRPN* intragenic CpG32	15	24346736	24347142	1	0.59	30	M
FAM50B	6	3849082	3850359	25	0.65	90	M	*SNRPN* intragenic CpG29	15	24671872	24672679	4	0.59	39	M
PLAGL1	6	144328078	144329888	16	0.58	143	M	*SNRPN* intragenic CpG30	15	24722753	24723071	1	0.66	29	M
IGF2R	6	160426558	160427561	2	0.70	74	M	*SNRPN* intragenic CpG40	15	25017924	25018886	4	0.51	67	M
GRB10	7	50848726	50851312	9	0.60	171	M	*ZNF597*	16	3481801	3482388	2	0.54	29	M
PEG10	7	94285537	94287960	53	0.60	119	M	*ZNF331*	19	54057086	54058425	4	0.66	102	M
MEST	7	130130122	130134388	55	0.54	226	M								
TRAPPC9	8	141108147	141111081	8	0.62	193	M	Novel DMRs (n = 6)							
INPP5F	10	121578046	121578727	4	0.59	52	M	*PPIEL*	1	40024626	40025540	4	0.54	39	M
H19	11	2018812	2024740	48	0.60	250	P	*WDR27*	6	170054504	170055618	2	0.56	58	M
IGF2 DMR2	11	2153991	2155112	9	0.65	63	P	*HTR5A*	7	154862719	154863382	6	0.62	55	M
IGF2 DMR0	11	2168333	2169768	1	0.62	33	P	*CXORF56 pseudogene/ ERLIN2*	8	37604992	37606088	7	0.45	37	M
KvDMR1	11	2719948	2722259	30	0.67	192	M	*WRB*	21	40757510	40758276	4	0.61	43	M
RB1	13	48892341	48895763	12	0.59	195	M	*NHP2L1*	22	42077774	42078873	8	0.54	63	M
IG-DMR	14	101275427	101278058	0	0.52	64	P								
MEG3	14	101290524	101293978	33	0.60	188	P	Known imprinted DMRs (n = 2) & novel DMRs (n = 15)							
MKRN3/ MIR4508	15	23807086	23812495	12	0.44	109	M	Placental-specific DMRs (n = 17)							
MAGEL2	15	23892425	23894029	6	0.55	51	M	*GPR1-AS*	2	207066967	207069445	3	0.49	86	M
NDN	15	23931451	23932759	8	0.65	108	M	*MCCC1*	3	182815725	182817627	13	0.54	94	M
SNRPN	15	25068564	25069481	8	0.42	19	M	*PDE4D*	5	58333774	58336554	7	0.54	145	M
SNRPN	15	25093008	25093829	4	0.49	44	M	*LIN28B*	6	105400631	105402559	8	0.45	62	M
SNRPN	15	25123027	25123905	5	0.47	45	M	*AIM1*	6	106957945	106961974	19	0.54	203	M
SNURF	15	25200004	25201976	7	0.60	113	M	*AGBL3*	7	134671024	134672011	12	0.59	74	M
IGF1R	15	99408496	99409650	7	0.51	55	M	*ZFAT*	8	135707227	135710114	3	0.60	111	M
ZNF597/ NAA60	16	3492828	3494463	11	0.54	76	P	*GLIS3*	9	4297279	4300182	9	0.63	235	M
ZNF331	19	54040510	54042212	11	0.64	125	M	*DCAF10*	9	37800140	37802937	5	0.56	157	M
PEG3	19	57348493	57353271	36	0.59	221	M	*FAM196A/DOCK1*	10	128993405	128995242	10	0.72	198	M
MCTS2P/HM13	20	30134663	30135933	9	0.48	47	M	*ZC3H12C*	11	109962727	109964784	9	0.66	198	M
BLCAP/NNAT	20	36148604	36150528	35	0.55	135	M	*N4BP2L1*	13	33000694	33002448	13	0.66	136	M
L3MBTL	20	42142365	42144040	25	0.65	84	M	*RGMA*	15	93614998	93616859	8	0.61	134	M
GNAS	20	57414039	57418612	23	0.57	257	P	*FAM20A*	17	66596155	66597643	4	0.72	162	M
NESP-AS/ GNAS-AS1	20	57425649	57428033	62	0.61	128	M	*ZNF396*	18	32956510	32957580	9	0.64	86	M
GNAS XL	20	57428905	57431463	6	0.65	200	M	*MIR512-1* cluster	19	54150515	54155608	6	0.53	216	M
GNAS Ex1A	20	57463265	57465201	38	0.67	198	M	*DNMT1*	19	10303506	10306415	10	0.55	129	M

The extent of imprinted methylation is defined by the size of the intermediately methylated region from the lymphocyte (for ubiquitous DMRs) and placenta (for placental-specific DMRs) WGBS data set.

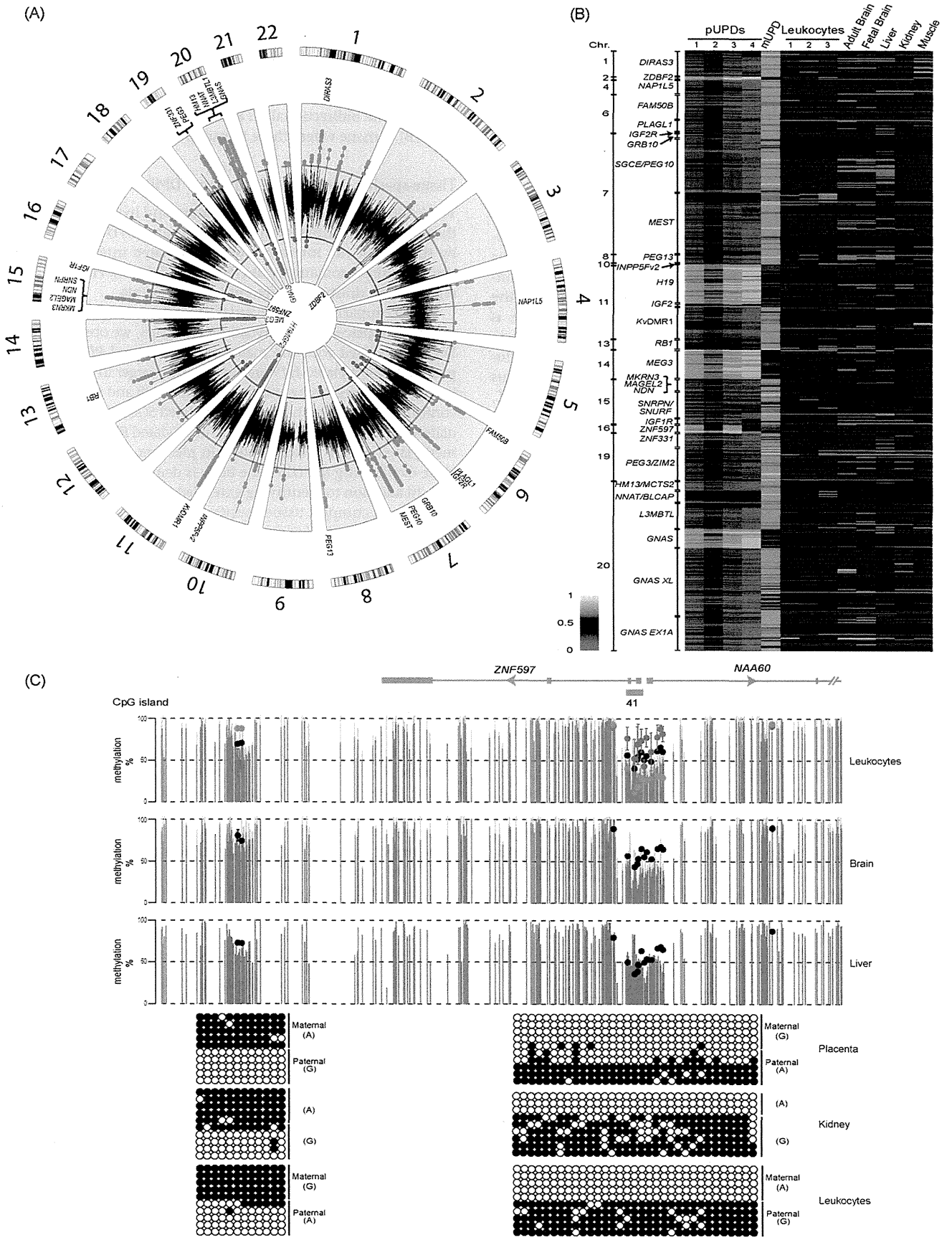

Figure 1. (Legend on next page)

all regions and verified that six regions (*PPIEL, WDR27, HTR5A, WRB, NHP2L1, ERLIN2* loci) are maternally methylated. The DMR we identify within intron 7 of *ERLIN2* appears to be a retroinsertion of the *CXorf56* pseudogene (also known as *LOC728024*) (Fig. 2B,C; Supplemental Fig. S3; Supplemental Table S1).

To confirm that parent-of-origin transcription occurs near these novel imprinted DMRs, we performed allelic RT-PCR in a panel of tissues with primers that discriminate major variant transcripts within each region. This revealed that the DMRs associated with *WDR27, NHP2L1,* and *CXorf56* pseudogenes regulate allelic expression in an isoform-specific fashion (Fig. 2B,C; Supplemental Fig. S3; Supplemental Table S1). We detect monoallelic expression of a short alternatively polyadenylated *ERLIN2* transcript which independently substantiates the observation that the generation of retrogenes, primarily from the X chromosome, is a common mechanism for generating imprinted loci (Wood et al. 2008; Kanber et al. 2009). Unfortunately, due to the lack of informative polymorphisms or expression in available heterozygous tissues, we could not perform allelic expression analysis for *PPIEL, HTR5A,* and *WRB.*

Histone methylation of H3K4 and DNA methylation are enriched on opposing alleles at imprinted DMRs

GC-rich sequences often coincide with enrichment of H3K4me3, which may act to protect them from de novo methylation (Thomson et al. 2010). The H3K4 demethylase KDM1B (previously known as AOF1) is required for appropriate establishment of maternal germline methylation for a subset of imprinted DMRs in mouse, suggesting that the presence of H3K4 methylation is refractory to DNA methylation deposition in the female germline (Ciccone et al. 2009). By comparing publicly available data sets for ChIP-seq for H3K4me3 and methylated DNA immunoprecipitation (meDIP-seq) from blood and brain, we observe co-enrichment of these opposing epigenetic marks at 89.5% of imprinted DMRs, consistent with differential active and repressive chromatin states on homologous chromosomes. For a limited number of informative regions, we were able to confirm H3K4me3 precipitation on the unmethylated allele (Fig. 3C). In most cases, the methylation profile of maternally methylated DMRs is more closely related to the opposing H3K4me3 profile rather than to the CpG density that classically defines CpG islands (>200 bp, GC content >50%, observed/expected ratio >0.6), with the exception of the *GNAS-XL* DMR. This maternally methylated region was thought to be a single regulatory unit; however, our WGBS and Infinium array data clearly show that it is two separate DMRs, partitioned by an ~200-bp interval of hypermethylation, with the centromeric *GNAS-AS1* (previously known as *NESP*-AS) promoter showing coenrichment for H3K4me3 and DNA methylation, while the *GNAS-XL* side lacks this permissive histone modification (Fig. 3A).

Further interrogation of this data set identified two DMRs associated with multiple promoters with a gradient effect across the CpG-rich sequences. The *GNAS/GNAS EX1A* CpG island (CpG island 320 in Fig. 3A) is unmethylated on one side, coinciding with H3K4me3, whereas the other is differentially methylated with abundant H3K4me3 and meDIP reads. This pattern was also observed in the bidirectional *HTR5A/HTR5A-AS1* promoter in brain (Fig. 3B), a tissue where these transcripts are most abundant.

Tissue-specific dynamics of imprinted DMRs

The WGBS analysis in leukocytes, brain, and liver confirmed that the extent of allelic methylation at the imprinted DMRs, as defined by the size of the intermediately methylated interval, is highly similar in these somatic tissues (Figs. 1, 4; Table 1). However, some regions were drastically different in the placenta.

By comparing the placental WGBS profile with Infinium β-values for placentae and hydatidiform moles, we observe that the DMRs associated with the maternally methylated *PEG10* and the paternally methylated *H19* are significantly larger in placenta than in somatic tissues. Using standard bisulfite PCR and sequencing, we confirm that the somatically unmethylated *SGCE* promoter, immediately adjacent to the differentially methylated *PEG10* promoter, is methylated on the maternal allele in placenta, while the maternal allele overlapping the *H19* gene body is demethylated (Fig. 4B).

In addition to identifying extended DMRs in the placenta, we also observe complex tissue-specific methylation between somatic tissues and placenta. For example, the *NNAT* and *GNAS-AS1* DMRs, which are maternally methylated in somatic tissue, exhibit hypermethylation in both placenta and hydatidiform mole. Subsequent bisulfite PCR confirmed that these regions are fully methylated in the placenta (Supplemental Fig. S4). Methylation profiling at the *MIR512-1* cluster (also known as *C19MC*)-*ZNF331* locus on chromosome 19 has previously disclosed that the promoter of the pri-miRNA for this miRNA cluster is maternally methylated in placenta, but fully methylated in somatic tissues (Noguer-Dance et al. 2010). We confirm that the *MIR512-1* DMR is unmethylated in hydatidiform moles compared to the partially methylated profile in placenta, with placental WGBS revealing that the DMR is ~5 kb in size, incorporating the promoter CpG island (CpG island 86 in Fig. 4C). However, we notice that the CpG island (CpG island 83 in Fig. 3C) associated with *ZNF331* isoform-3 is hypermethylated on both parental alleles in placenta but is a maternally methylated DMR in somatic tissues. These methylation states dictate complex allelic expression at this locus, with restricted placental-specific paternal expression of the *MIR512-1* pri-miRNA, which does not extend to the *MIR371/2* cluster, and reciprocal imprinting of *ZNF331* (Fig. 4C; Supplemental Table S2).

Novel placental-specific DMRs associated with paternally expressed transcripts

Based on the complex methylation profiles described above, we next investigated if more unknown imprinted DMRs exist solely in

Figure 1. Identification of known imprinted DMRs on the Infinium array platform. (*A*) Circular karyotype showing the difference of methylation for three consecutive probes for reciprocal UPD leukocyte samples. Red dots indicate a minimal difference of 0.3 in Infinium probe β-values (>30% absolute methylation value) for regions with maternal methylation, and blue dots indicate the same for paternal methylation. Known DMRs are indicated. (*B*) Heat map of the Infinium probes located within known imprinted DMRs in reciprocal genome-wide UPD samples and various somatic tissues. (*C*) WGBS and Infinium array methylation profiles of the *ZNF597* locus with bisulfite PCR confirmation of the novel maternally methylated DMR and its position in relation to the somatic paternally methylated promoter region. Vertical gray lines in the WGBS tracks represent the mean methylation value for individual CpG dinucleotides calculated from multiple data sets, with the light gray lines representing the mean + standard deviation. Infinium methylation values for normal tissues are represented by black dots, with values for the genome-wide UPDs (average pUPD in blue and mUPD in red) superimposed on the leukocyte methylation track. The error bars associated with the Infinium array probes represent the standard deviation of multiple biological samples. The PCR confirmation in placenta, kidney, and leukocyte-derived DNA was performed on heterozygous samples. Each circle represents a single CpG dinucleotide on a DNA strand. (●) Methylated cytosine, (○) unmethylated cytosine. Each row corresponds to an individual cloned sequence.

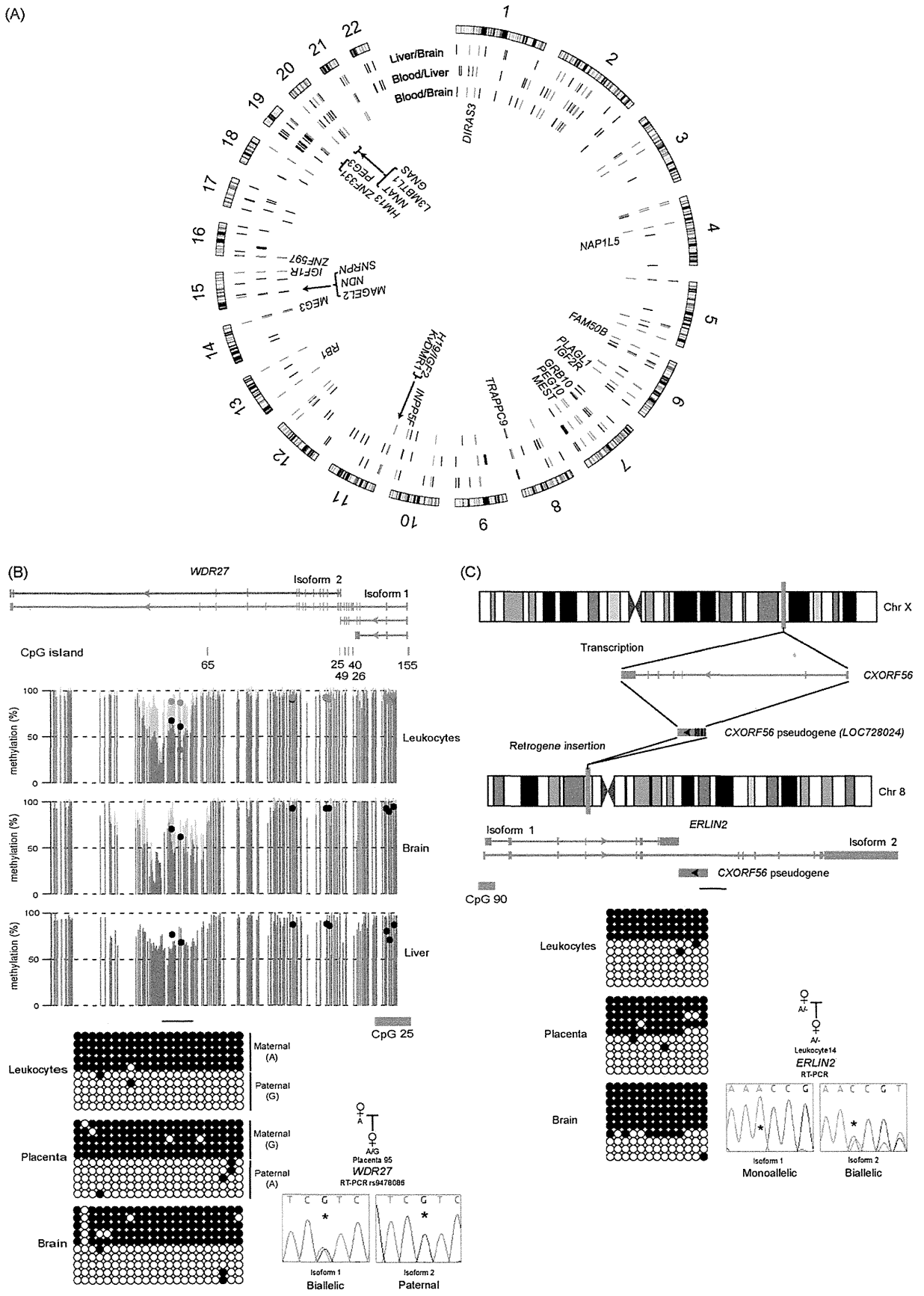

Figure 2. (Legend on next page)

placental tissues, as highlighted by the *MIR512-1* and *GPR1-AS* DMRs (Noguer-Dance et al. 2010; Kobayashi et al. 2013).

We performed a screen for partially methylated regions present solely in our placenta WGBS data set using our sliding window approach (0.25 < mean of 25 CpG ± 2 SD < 0.75). This identified 722 windows, of which 520 mapped to CpG islands. These results confirm that placental-derived DNA is significantly less methylated when compared to other tissues (Schroeder et al. 2013) and that this genome-wide lower methylation is not restricted to repetitive elements as previously described (Ehrlich et al. 1982; Fuke et al. 2004), but occurs across a large portion of the genome.

Of these partially methylated placenta domains identified by WGBS, 44 regions were ~50% methylated in placenta, with extreme methylation in hydatidiform moles using the Infinium array (average β-value for three consecutive probes >0.8 indicative of paternal methylation or <0.2 indicative of maternal methylation), and showed no evidence of allelic methylation in somatic tissues. Using standard bisulfite PCR, we assessed the allelic methylation profile of all regions in placental DNA samples. This revealed that the promoters of *N4BP2L1, DCAF10, PDE4D, FAM196A, RGMA, AGBL3, MCCC1, ZC3H12C, DNMT1, AIM1, ZNF396, FAM20A, GLIS3*, and *LIN28B* are methylated on the maternal allele (Fig. 4D; Supplemental Fig. S5; Supplemental Table S2). In addition, we identified a 2.8-kb region of intermediate methylation overlapping an alternative promoter of the paternally expressed *ZFAT* gene in the placental WGBS data set (Supplemental Fig. S5). Using allelic-specific bisulfite PCR, we confirm that the methylation is confined to the maternal chromosome at this locus. To determine if these regions of maternal methylation influence transcription, allelic RT-PCR experiments were carried out. Paternal expression of eight of these genes was verified, with biallelic expression in somatic tissues (Fig. 4D; Supplemental Fig. S5; Supplemental Table S2) consistent with recent allelic expression screens in term placenta (Yuen et al. 2011; Barbaux et al. 2012).

Mammalian conservation of novel imprinted domains

To determine if the previously unrecognized imprinted domains are conserved throughout evolution, we assessed their allelic methylation and expression in mice, using a reciprocal cross between mouse strains. Bisulfite PCR targeting of orthologous regions failed to identify evidence of differential methylation in embryonic day E9.5–14.5 embryos or extra-embryonic tissues. Subsequent allelic RT-PCRs revealed that all murine transcripts orthologous to the novel ubiquitous and placental-specific imprinted transcripts are equally expressed from both parental alleles when detected (Supplemental Figs. S6, S7). This suggests that these new imprinted domains arose less than ~80 million years ago after the divergence of mice and humans or that selection pressures over this period have resulted in a loss of imprinted regulation of these genes in mice. It has been previously reported that imprinting in the placenta differs between human and mouse, mainly due to the lack of imprinting of genes which require repressive histone modifications for allelic silencing in humans (Monk et al. 2006). Contrary to previous reports, our results show that humans have evolved more loci subject to this form of transcriptional regulation in placenta, due to the evolutionary acquisition of loci with parent-of-origin methylation. This is endorsed by the low discovery rate of novel imprinted transcripts in RNA-seq screens of mouse placenta (Okae et al. 2011).

Differential methylation at ubiquitously imprinted loci and placental-specific domains may differ in their gametic origin

An essential step toward understanding the establishment of the germline imprint signal is to determine if the parent-of-origin methylation observed in somatic tissues is derived from the germline. Determining the methylation profiles in human gametes and during the early preimplantation stages of embryonic development is technically and ethically challenging. To circumvent these difficulties, we have used a combination of mature gametes and in vitro models to represent human gametes of both sexes and preimplantation embryos. For analysis during gametogenesis in males, we used mature sperm. We compared publicly available WGBS data sets from sperm and human embryonic stem (hES) cells that represent the inner cell mass of the blastocysts (Lister et al. 2009; Molaro et al. 2011) with our own Infinium array profiles for sperm, parthenote-derived hES cell lines (phES), and hES cell lines generated from both six-cell blastomeres (Val10B) and the inner cell mass of blastocysts (SHEF cell lines). Despite the phES cell lines having undergone reprogramming during blastocyst development, they have previously been shown to retain maternal hypermethylation at the limited imprinted loci assessed, suggesting that they are ideal surrogates for assessing the methylation profiles of imprinted DMRs in mature oocytes (Mai et al. 2007; Harness et al. 2011).

A comparison of Infinium β-values between sperm and phES cells for the human sequences orthologous to the mouse germline DMRs (Kobayashi et al. 2012) revealed that 19/22 are conserved. The novel ubiquitous DMRs we identify are also hypermethylated in phES cells and unmethylated in sperm, suggesting that the majority of imprinted DMRs, with the exception of *IGF1R*, are primarily marked in the gametes (Fig. 5A; Supplemental Fig. S8). In addition, we confirm that the IG-DMR within the chromosome 14 domain is >80%–90% methylated in the sperm WGBS data set, in line with previous reports (Geuns et al. 2007). We were particularly intrigued to observe that all placental-specific DMRs, with the exception of *ZFAT, GPR1-AS*, and *MIR512-1*, do not inherit methylation from the gametes and are devoid of methylation in hES cells (Fig. 5A). These data provide preliminary evidence to suggest that, following gametogenesis, parental alleles at some loci retain a nonequivalency that is not associated with DNA methylation.

Figure 2. Identification and characterization of allelic methylation and expression of novel imprinted loci. Circular karyotype showing the position of common regions of intermediate methylation in the leukocyte, brain, and liver WGBS data sets, as identified using a 25 CpG sliding window approach (0.25 < mean ± 1.5 SD < 0.75). Red ticks represent sites of intermediate methylation common to all tissues, whereas black ticks identify those present in only one or two pairwise comparisons. The position of known imprinted DMRs are shown. (*B*) Identification of a novel maternally methylated DMR within the *WDR27* locus by WGBS and Infinium array analysis. Vertical gray lines in the WGBS tracks represent the mean methylation value for individual CpG dinucleotides calculated from multiple data sets, with the light gray lines representing the mean + standard deviation. Infinium methylation values for normal tissues are represented by black dots, with values for the genome-wide UPDs (average pUPD in blue and mUPD in red) superimposed on the leukocyte methylation track. The DMR was confirmed using standard bisulfite PCR on heterozygous DNA samples and orchestrates paternal expression of *WDR27* isoform 2. The asterisk (*) in the sequence traces shows the position of the polymorphic base. (*C*) Imprinting of *ERLIN2* isoform 1 in leukocytes as a consequence of the retrotransposition of the X chromosome-derived *CXorf56* pseudogene into the locus.

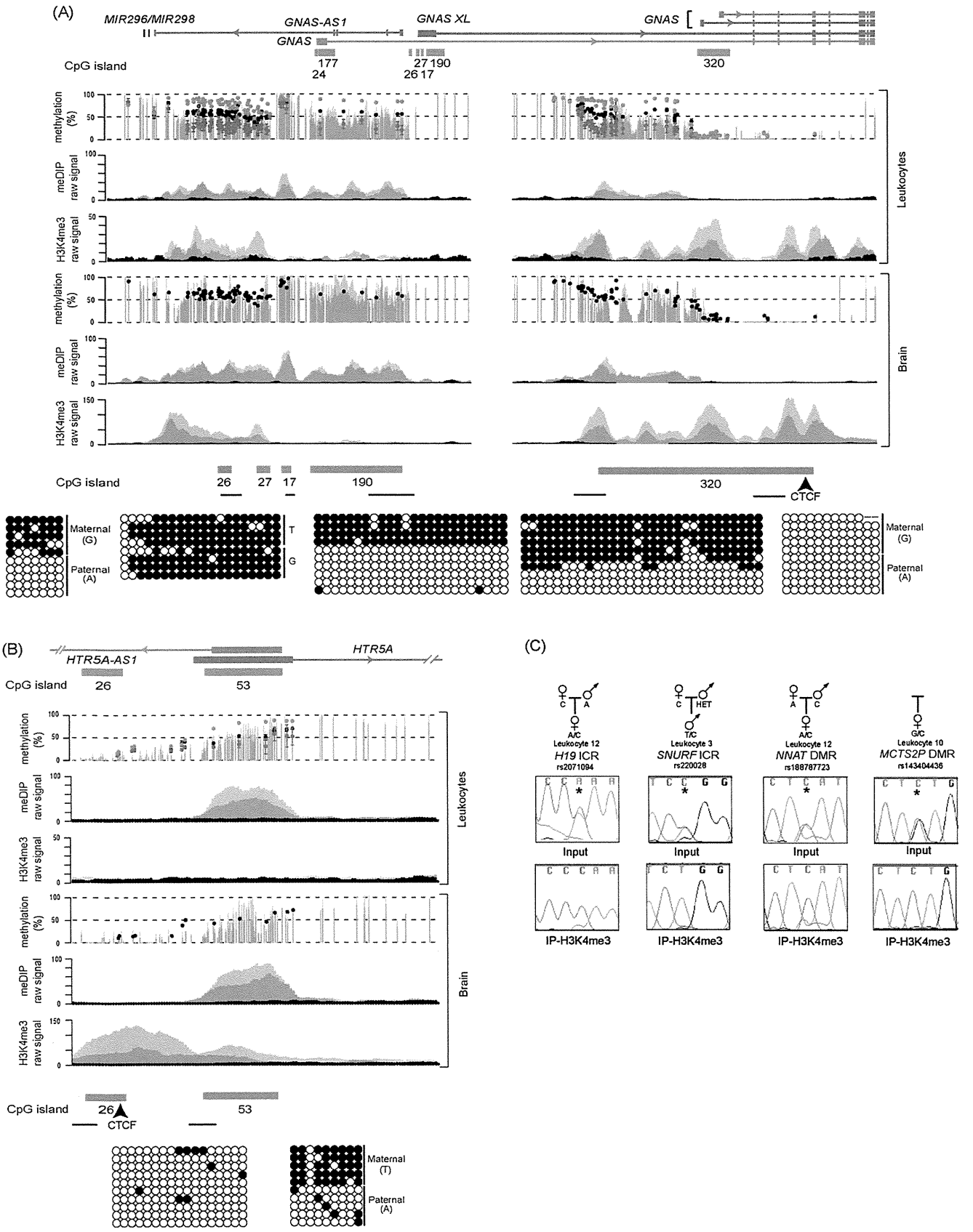

Figure 3. H3K4me3 chromatin profile and DNA methylation at imprinted loci. (*A*) Map of the human *GNAS* locus on chromosome 20 with the H3K4me3 and meDIP signatures in brain and leukocytes at the DMRs identified in the WGBS and Infinium array analysis. Infinium methylation values for normal leukocytes (black dots), with values for the genome-wide pUPD (blue) and mUPD (red) superimposed on the leukocyte WGBS track. Similarly, Infinium methylation values for two normal brain samples are shown as black and gray dots. The light and dark gray peaks in the meDIP and ChIP-seq panels represent two independent biological replicates compared to input (black peaks). The bars *under* the CpG islands, as identified in the UCSC Genome Browser, show the location of the bisulfite PCR amplicons. (*B*) The gradient DMR identified at the *HTR5A* promoter. The samples used for the WGBS, Infinium array, and ChIP are the same as in *A*. The independent methylation pattern on either side of the bidirectional promoter interval was confirmed using standard bisulfite PCR and sequencing. (*C*) Allelic ChIP for H3K4me3 reveals predominant enrichment of this histone modification on the unmethylated allele of the *H19* ICR, *SNURF* ICR, *NNAT*, and *MCTS2P* DMRs. The asterisk (*) in the sequence traces shows the position of the polymorphic base.

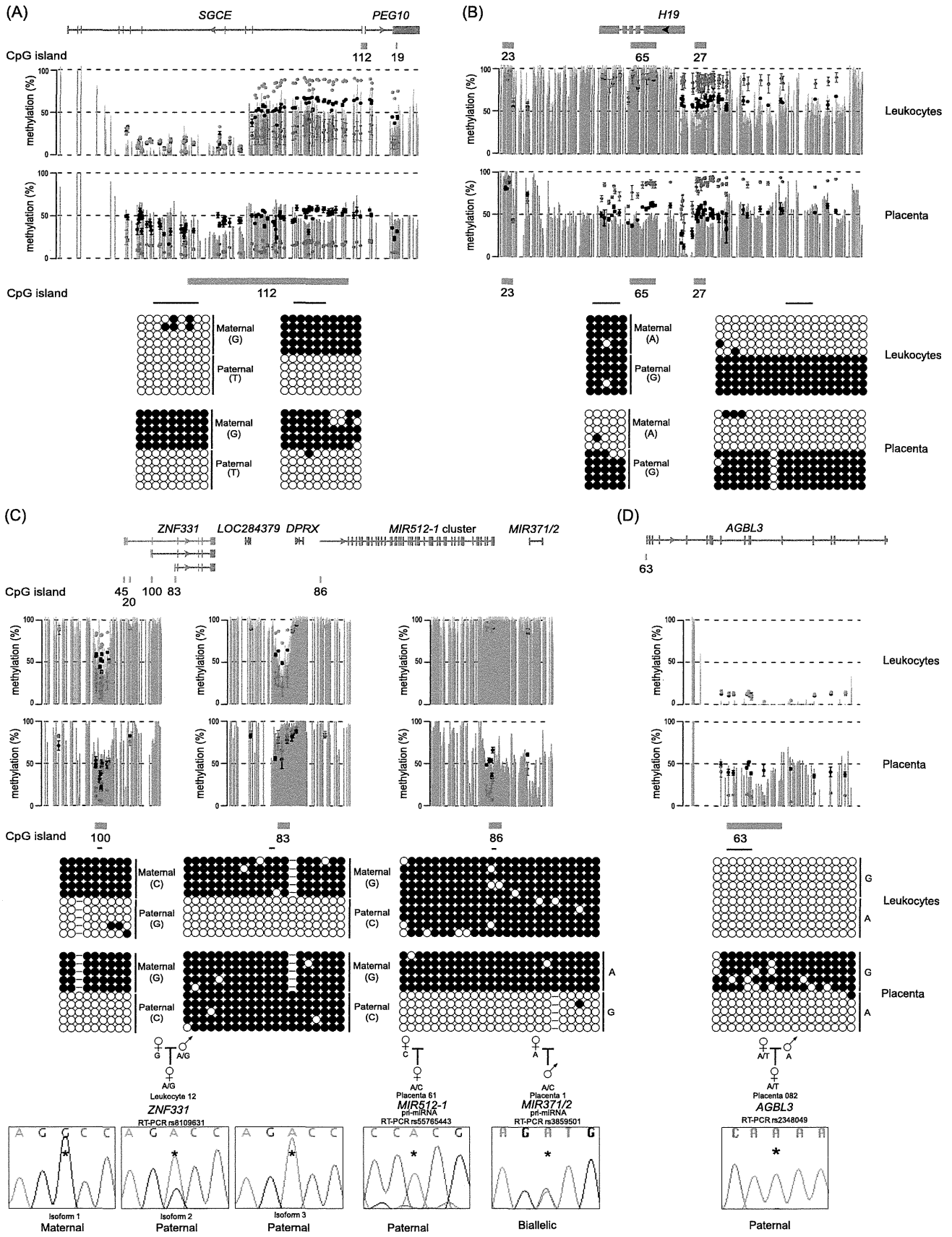

Figure 4. (Legend on next page)

Therefore, in the female germline, as represented by the phES cells, a subset of imprinted loci retain their identity in the absence of methylation, suggesting that additional epigenetic mechanisms mark these regions for maternal methylation during trophoblast differentiation (Fig. 5A).

For the majority of DMRs for which allelic methylation was observed in the somatic tissues (80%), the genomic interval showing methylation differences between sperm and phES cells is larger than the allelic DMRs in hES cells and somatic tissues (Fig. 5B,C). In the case of maternally methylated DMRs, we observe that these regions are flanked by fully methylated intervals in both gametes, and that these DMRs are observed as regions devoid of methylation in the sperm genome. Interrogation of ChIP-seq data sets for nucleosomes containing the histone modifications revealed that the majority of unmethylated DMR regions in sperm are enriched for H3K4me3 containing nucleosome fractions. Our analysis indicates that the size of the unmethylated region in sperm is therefore associated with nucleosome occupancy, rather than protamines. Notably, the maternally methylated germline DMR overlapping the *NNAT* promoter is ~4 kb, as defined by full methylation in phES cell and the H3K4me3 enriched DNA unmethylated region in sperm. This region contracts to an ~1.5-kb region of maternal methylation after preimplantation reprogramming as represented by blastocyst-derived hES cells and somatic tissue profiles (Fig. 5C; Supplemental Fig. S9A showing the contraction at the *NAP1L5* locus). Such resizings are also observed in mouse (Tomizawa et al. 2011), suggesting that imprinted DMRs are not totally protected from genome-wide demethylation during the oocyte to embryo transition. We speculate that the larger regions of differential methylation dictated by the gametes, in combination with protective factors, ensure that they survive reprogramming.

In addition, we also observe other subtle differences in germline-derived methylation profiles. For example, the two sides of the *GNAS-XL* DMR that we show to have independent H3K4 methylation profiles from each other behave differently in the germline, with the *GNAS-AS1* side being a somatic DMR only, but the *GNAS-XL* side being methylated in phES cells and hypomethylated in sperm (Supplemental Fig. S4). Lastly, we identified a dynamic relocalization of methylation at the *FAM50B* DMR during preimplantation development. The 1.2-kb promoter of this imprinted retrogene is methylated on the maternal allele in somatic tissues but is completely unmethylated in phES cells and hES cells derived from six-cell embryos, and has been shown to be unmethylated in sperm (Nakabayashi et al. 2011). However, we do find that allelic methylation is conferred during preimplantation development, at a point between the six-cell stage and blastocyst development. In fact, the ~1-kb regions flanking the promoter (labeled 1 and 3 in Supplemental Fig. S9B) show strongly opposing methylation profiles, with the sperm being unmethylated and phES cells methylated, which then become fully methylated on both alleles immediately after fertilization, leaving allelic methylation over the promoter itself.

Discussion

Differentially methylated regions between the parental alleles are essential for genomic imprinting and development. In this study, we have performed a comprehensive survey of methylation in various human tissues, uncovering all known imprinted DMRs as well as 21 novel loci, which we demonstrate wherever possible regulate imprinted transcription. Our present work demonstrates that the human genome contains a significantly larger number of regions of parent-of-origin methylation than previously thought. The identification of imprinted domains has traditionally been performed in mouse by utilizing gynogenetic and androgenetic embryos, mice harboring regions of uniparental disomies, or highly polymorphic inbred strains (Cooper and Constância 2010). These embryos have been subjected to expression-based screens, including RNA-seq (Gregg et al. 2010; Okae et al. 2011), and genome-wide methylation techniques (Hayashizaki et al. 1994; Kelsey et al. 1999; Hiura et al. 2010). By relying on the confirmation of the evolutionarily conserved expression of the human orthologs, imprinted genes specific to higher primates and humans would have been missed. We have utilized high-throughput bisulfite analysis from in vitro models of gametes and early embryos, and somatic and placental DNA, to characterize the developmental dynamics of imprinted methylation coupled with allelic expression analysis of nearby transcripts. This analysis reveals that 30 regions of parentally inherited differential methylation are observed in humans but not mice. Conversely, we also show that the DMRs associated with *Cdkn1c*, *Rasgrf1*, the *Igf2r* promoter, *Impact*, *Slc38a4*, and *Zrsr1* (previously known as *U2af1-rs1*) imprinted transcripts in mouse do not exhibit allelic methylation in humans (Xie et al. 2012).

Recently, a novel mechanism has been described in which differences in germline methylation can give rise to tissue-specific DMRs in mouse (Proudhon et al. 2012). The *Cdh15* DMR inherits methylation from the oocyte and maintains this parental allelic methylation during in utero development and in adults, with the exception that the paternal allele gains methylation in various brain regions. Therefore, the intragenic *Cdh15* DMR is conserved during adulthood, but in a tissue-specific manner. In humans, the *CDH15* locus does not exhibit allelic DNA methylation in any tissue (data not shown), suggesting that this tissue-specific methylation profile might be limited to mice. We cannot rule out the existence of temporally regulated tissue-specific imprinted DMR in humans, since our samples were derived from adults, and therefore any imprinted DMRs specific to the fetal period would be missed.

Our study reveals the power of combining WGBS and Infinium HumanMethylation450 BeadChip arrays to identify novel imprinted DMRs. We have previously combined reciprocal genome-wide UPD samples and the Infinium HumanMethylation27

Figure 4. The methylation profiles of imprinted loci in placenta compared to somatic tissues. The placenta- and leukocyte-derived WGBS and Infinium array profiles at the (*A*) *PEG10* and (*B*) *H19* loci. Infinium methylation values for normal leukocytes (black dots), with values for the genome-wide pUPD (blue) and mUPD (red) superimposed on the leukocyte WGBS track. Similarly, Infinium methylation values for normal placenta (black dots) and hydatidiform mole (blue dots) are overlaid on the placental WGBS track. The error bars associated with the Infinium array probes represent the standard deviation of multiple biological samples. Bisulfite PCR analysis was used to confirm the tissue-specific methylation profiles. (*C*) Complex tissue-specific allelic methylation and expression patterns at the *ZNF331-MIR512* cluster locus on chromosome 19. The *ZNF331* sequence traces represent the RT-PCR products from leukocytes, whereas both the *MIR512-1* cluster and *MIR371/2* are from placenta. (*D*) A placental-specific imprinted DMR identified using the placenta-derived WGBS and Infinium array data sets. The methylation profiles were confirmed using standard bisulfite PCR on heterozygous DNA samples with allelic RT-PCR performed on placental biopsies. The results confirm that the region of maternal methylation overlapping the *AGBL3* promoter dictates paternal expression of this gene in placenta.

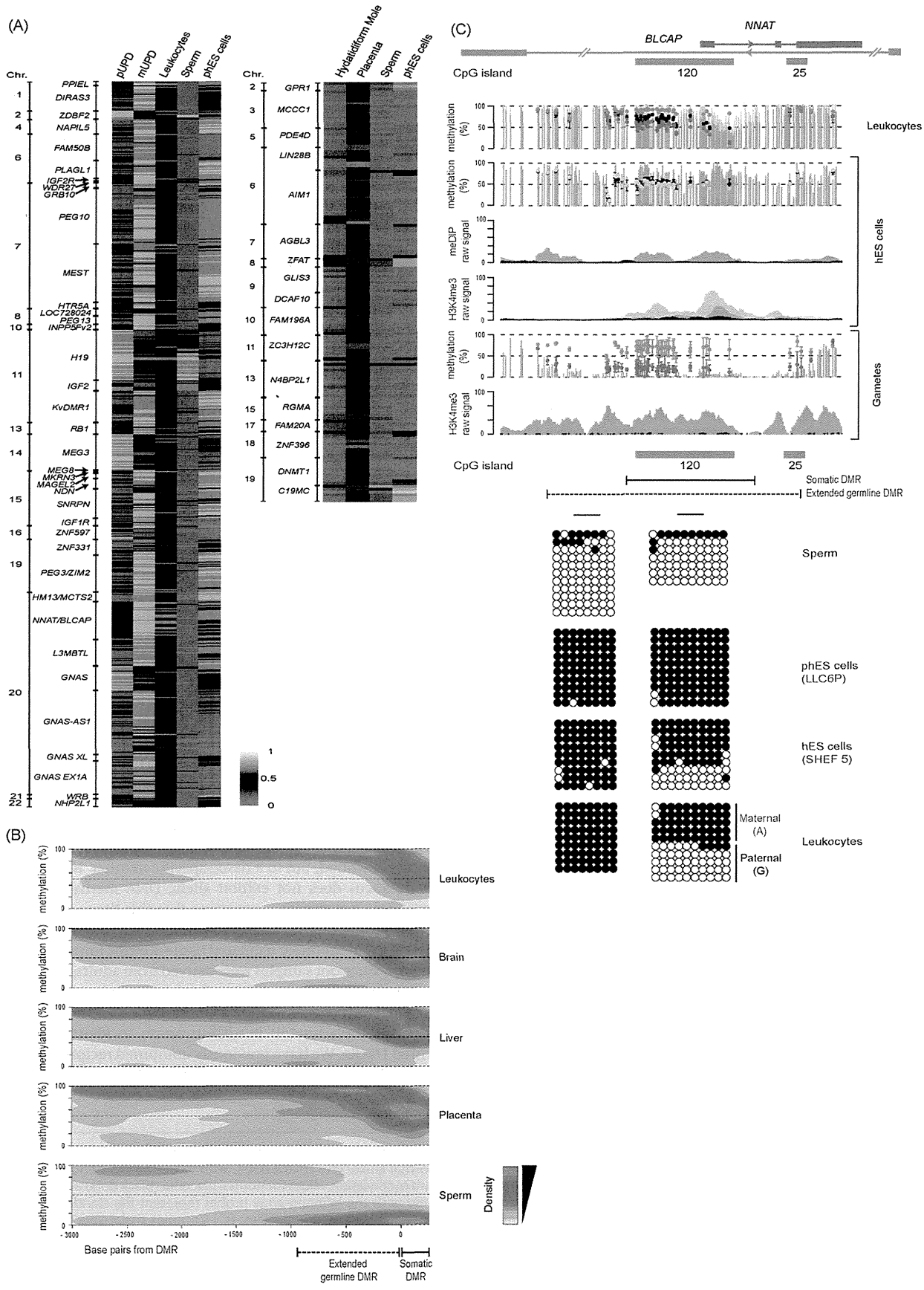

Figure 5. (Legend on next page)

BeadChip arrays to identify imprinted loci (Nakabayashi et al. 2011). All new regions of ubiquitous imprinted methylation identified in the current screen are associated predominantly with type II Infinium probes and were not present on previous array platforms. Of the placental-specific DMRs, only those associated with *DNMT1, AIM1,* and *MCCC1* have been previously described (Yuen et al. 2011; Das et al. 2013). Intriguingly, the somatic promoter of *Dnmt1* is differentially methylated between sperm and oocytes but is lost during preimplantation development (Smallwood et al. 2011; Kobayashi et al. 2012). Two of these placental-specific DMRs are associated with type I Infinium probes and were previously discovered using the Infinium HumanMethylation27 BeadChip arrays with DNA derived from diandric and digynic triploid placental samples (Yuen et al. 2011).

Our data provide the first direct evidence in humans that the differential methylation associated with imprinted genes is dynamically regulated upon fusion of the gametes at fertilization. Most maternally methylated DMRs are surrounded by regions of complete methylation in both gametes, and as in mice, the DMRs are clearly observed as unmethylated islands in the sperm genome. These unmethylated intervals are often more extensive in sperm compared to somatic tissues, suggesting that resizing occurs during embryonic transition. It was recently reported that nucleosomes are retained at specific functional regions in sperm chromatin and are refractory to protamine exchange (Hammoud et al. 2009). These sperm-derived histones are enriched for H3K4me3, a permissive modification that is mutually exclusive with DNA methylation, implicating these H3K4me3 regions in the maintenance of the unmethylated state in the male germline.

Imprints are distinguishable from other forms of gametic methylation as they survive the reprogramming that initiates immediately upon fertilization (Smallwood et al. 2011; Kobayashi et al. 2013; Proudhon et al. 2012). By comparing the profiles of sperm, phES, and conventional hES cells along with somatic tissues, we present evidence that most maternally methylated DMRs are not completely refractory to reprogramming, as highlighted by the substantial resizing of the paternally derived unmethylated alleles. These data are consistent with the notion that the cores of imprinted DMRs are protected from Tet-associated demethylation by recruiting heterochromatic factors such as ZFP57 and DPPA3 (also known as STELLA or PGC7) (Nakamura et al. 2007; Li et al. 2008). Similar mechanisms could also act to protect the core of the unmethylated paternal alleles from methylation.

A search for the mouse ZFP57 recognition sequence ($TGCC^{met}GC$) identified numerous binding sites within the ubiquitous imprinted DMRs that may be involved in protecting methylation during preimplantation reprogramming (Quenneville et al. 2011). It is currently unknown if this hexonucleotide motif is bound by ZFP57 in human cells, but patients with mutated ZFP57 lack DNA binding capacity in in vitro EMSA studies (Baglivo et al. 2013).

There are significantly fewer ZFP57 sequence motifs in the placental-specific DMRs compared to the ubiquitous DMRs that inherit methylation from the germline ($P < 0.05$, Student's *t*-test), with 14/17 placental-specific DMRs being unmethylated and not associated with H3K9me3 in hES cells (Supplemental Fig. S10). These data further support our hypothesis that a novel imprinting mechanism occurs in the placenta, which is one of the first examples of methylation-independent epigenetic inheritance in mammals. In support of our observations, Park and colleagues (Park et al. 2004) generated a *H19* ICR knock-in at the *Afp* locus which was de novo methylated around gastrulation, implying that *H19* ICR is differentially marked in the gametes by a mechanism other than methylation. However, it is unknown if this mechanism also occurs at the endogenous *H19* locus. In our examples of placental-specific DMRs, the epigenetic mark inherited from the oocyte is currently unknown, but must be recognized by the de novo methylation machinery during early trophoblast differentiation, since we observe maternal methylation in term placenta. Certain histone methylation states are reported to recruit DNMTs (Dhayalan et al. 2010; Zhang et al. 2010). Since various post-translational modifications of histone tails have been shown to be present at imprinted loci, specifically in the placenta independent of DNA methylation (Umlauf et al. 2004; Monk et al. 2006), we are led to suggest one inviting hypothesis: A histone modification confers the "imprint" at these novel placental-specific imprinted loci. Alternatively, the DNMTs may be recruited to these loci by a specific, yet to be identified, transcription factor expressed during early trophoblast differentiation.

In line with other well-characterized imprinted genes in the placenta, the placental-specific imprinted transcripts may also exert supply-and-demand forces between the developing fetus and mother, ultimately influencing fetal adaptation in utero, which if disrupted may have long-term consequences on health many decades after delivery (Constância et al. 2004). Our observation of imprinting of the somatic promoter of *DNMT1* in placenta may therefore assist in this process. In addition, numerous studies have also suggested that children born as a result of assisted reproductive technologies (ART), including ovarian stimulation, in vitro fertilization, and intra-cytoplasmic sperm injections, have a higher risk of diseases with epigenetic etiologies, including imprinting disorders (Amor and Halliday 2008). In a clinical context, the placenta-specific imprinted loci may be prone to epigenetic instability during ART, as the first differentiation step that results in the trophectoderm occurs when the developing blastocysts are in culture.

By utilizing genome-wide methylation profiling at base-pair resolution, we have catalogued regions of parentally inherited methylation associated with imprinted regions and highlighted all differences between somatic and placental tissues. Further studies of these loci will provide insight into the causes of epigenetic ab-

Figure 5. Methylation in gametes, hES cells, and somatic tissues. (*A*) Heat maps for Infinium probes mapping within all ubiquitous (*left*) and placental-specific (*right*) imprinted DMRs in sperm and phES cells reveal the germline acquisition of methylation. (*B*) Methylation contour plots from WGBS data sets for all maternally methylated DMRs reveal that the extent of the intermediately methylated regions associated with imprinted DMRs are extremely consistent between somatic tissues and significantly larger in sperm. (*C*) Methylation profiles at the *NNAT* DMR determined by WGBS, Infinium array, and meDIP-seq data sets in leukocytes, sperm, phES cells, and hES cells, along with the H3K4me3 ChIP-seq reads for hES cells and sperm. The gray and black dots in the second panel represent Infinium probe methylation in hES cell lines derived from six-cell blastomeres (Val10B) and blastocytes (SHEF5), respectively. The gametic WGBS methylation profile is derived from sperm, with Infinium probe methylation values for sperm and phES cells represented by blue and red dots. The graphic shows the extent of the differentially methylated regions in somatic tissues and between sperm and phES cells. The error bars associated with the Infinium array probes represent the standard deviation of the two sperm samples and four independent phES cell lines. The H3K4me3 ChIP-seq data is from sperm. The methylation profiles were confirmed using standard bisulfite PCR and sequencing.

errations associated with imprinting disorders and may be relevant to the epigenetic causes of common diseases.

Methods

Tissue samples and cell lines

Peripheral blood was obtained from healthy volunteers or from the umbilical cord of newborns for which we obtained matched placental biopsies. These samples were collected at the Hospital St. Joan De Deu (Barcelona, Spain) and the National Center for Child Health and Development (Tokyo, Japan). All placenta-derived DNA samples were free of maternal DNA contamination based on microsatellite repeat analysis. The brain samples were obtained from BrainNet Europe/Barcelona Brain Bank. Ethical approval for this study was granted by the Institutional Review Boards at the National Center for Child Health and Development (project 234), Saga University (21-5), Hamamatsu University School of Medicine (23-12), Hospital St. Joan De Deu Ethics Committee (35/07), and Bellvitge Institute for Biomedical Research (PR006/08). Written informed consent was obtained from all participants.

The hES (SHEF 3, 5, 6 and Val10B) and parthenogenetically activated oocyte (LLC6P, LLC7P, LLC8P, and LLC9P) cell lines were used because they were epigenetically stable at imprinted loci (with the exception of *NNAT* LOM and *GNAS* GOM in LLC7P; LOM of *PEG3* in Val10B; GOM of *MCTS2P* in SHEF3) and grown as previously described (Harness et al. 2011). Ethical approval for the study of these cells was granted by the Bellvitge Institute for Biomedical Research Ethics Committee (PR096/10) and Comité Ético de Investigación Clínica (CEIC) del Centro de Medicina Regenerativa de Barcelona-CMR[B] (28/2012) and complied with the legal guidelines outlined by the Generalitat de Catalunya El conseller de Slaut.

Wild-type mouse embryos and placentae were produced by crossing C57BL/6 (B) with *Mus musculus molosinus* (JF1) or *Mus musculus castaneous* (C) mice. Mouse work was approved by the Institutional Review Board Committees at the National Center for Child Health and Development (approval number A2010-002). Animal husbandry and breeding were conducted according to the institutional guidelines for the care and the use of laboratory animals. DNA and RNA extractions and cDNA synthesis were carried out as previously described (Monk et al. 2006).

Characterization of the genome-wide UPD samples

Genomic DNA was isolated from two previously described genome-wide paternal UPD cases with BWS features (Romanelli et al. 2011) and two newly identified individuals, at Saga University, as well as one genome-wide maternal UPD with a SRS phenotype (Yamazawa et al. 2010). Each of these cases had undergone extensive molecular characterization to confirm genome-wide UPD status and the extent of mosaicism. We used DNA isolated from lymphocytes, as these samples had minimal contamination of the biparental cell lines. The genome-wide pUPD samples had 9, 11, 9, and 2% biparental contribution, whereas the genome-wide SRS sample had 16%. In addition, four hydatidiform moles were collected by the National Center for Child Health and Development.

Genome-wide methylation profiling

We analyzed six publicly available methylomes, including those derived from CD4+ lymphocytes (GSE31263) (Heyn et al. 2012), brain (GSM913595) (Zeng et al. 2012), the H1 hES cell line (GSM432685, GSM432686, GSM429321, GSM429322, GSM429323), and sperm (GSE30340). In addition, we generated three additional tissue methylomes using WGBS for brain, liver, and placenta. WGBS libraries were generated as previously described (Heyn et al. 2012).

We also generated methylation data sets using the Illumina Infinium HumanMethylation450 BeadChip arrays, which simultaneously quantifies ~2% of all CpG dinucleotides. Bisulfite conversion of 600 ng of DNA was performed according to the manufacturer's recommendations for the Illumina Infinium Assay (EZ DNA methylation kit, Zymo). The bisulfite-converted DNA was used for hybridization following the Illumina Infinium HD methylation protocol at genomic facilities of the Cancer Epigenetics and Biology Program (Barcelona, Spain) or the National Center for Child Health and Development. Data was generated for the genome-wide UPDs (4× pUPD, 1× mUPD), two brain, one liver, one muscle, one pancreas, two sperm, four hydatidiform moles, four term placentae, four phES cell lines, and the four hES lines. In addition, we used three leukocyte data sets from GSE30870.

Data filtering and analysis

For WGBS, the sequence reads were aligned to either strand of the hg19 reference genome using a custom computational pipeline (autosomal CpGs with at least five reads: brain sample, 190,314,071 aligned unique reads, 83% coverage; liver sample, 778,733,789 aligned unique reads, 96.6% coverage; placenta sample, 319,362,653 aligned unique reads, 89.6% coverage). The methylation level of each cytosine within CpG dinucleotides was estimated as the number of reads reporting a C, divided by the total number of reads reporting a C or T. For the identification of intermediately methylated regions associated with imprinted DMRs, we performed a sliding window approach in which the methylation of 25 CpGs was averaged after filtering for repetitive sequences. The location of these sequences was taken from the UCSC sequence browser. An interval was considered partially methylated if the average methylation was $0.25 < \text{mean} \pm 1.5\ \text{SD} < 0.75$.

For the Illumina Infinium HumanMethylation 450 BeadChip array, before analyzing the data, we excluded possible sources of technical biases that could influence results. We applied signal background subtraction, and inter-plate variation was normalized using default control probes in BeadStudio (version 2011.1_Infinium HD). We discarded probes with a detection *P*-value >0.01. We also excluded probes that lacked signal values in one or more of the DNA samples analyzed. In addition, we discarded 16,631 probes as they contained SNPs present in >1% of the population (dbSNP 137). Lastly, prior to screening for novel imprinted DMRs, we excluded all X chromosome CpG sites. In total, we analyzed 442,772 probes in all DNA samples. All hierarchical clustering and β-value evaluation was performed using the Cluster Analysis tool of the BeadStudio software.

In-house R-package scripts were used to evaluate the average methylation of three contiguous Infinium probes. To identify regions with potential allelic methylation, we screened the reciprocal genome-wide UPDs for three consecutive probes with an average β-value difference greater than 0.3 (Limma linear model $P < 0.05$):

$$\left|\frac{1}{3}\sum_{n=0}^{2} pUPDs_n - \frac{1}{3}\sum_{n=0}^{2} mUPD_n\right| > 0.3.$$

With the condition that the average of three consecutive probes for the normal leukocytes is between the values for the reciprocal genome-wide UPDs: